I - B 159

IDENTIFICATION OF SOIL-STRUCTURE-INTERACTION EFFECT FROM EARTHQUAKE RECORDS AT TWO BASE-ISOLATED BRIDGES IN CLOSE VICINITY

University of Tokyo	Student Member	M. Tariq Amin CHAUDHARY
University of Tokyo	Member	Masato ABE
University of Tokyo	Fellow	Yozo FUJINO

1- Introduction: Identification of system parameters with the help of records made on base-isolated bridge during earthquakes provide an excellent opportunity to study the performance of the various components of such bridge system. This study utilizes a system identification methodology developed earlier by the authors [1] to reliably identify structural parameters of such bridges from recorded acceleration data. Application of this methodology to two base isolated bridges which were shaken by the 1995 Kobe earthquake enabled to examine soil-structure interaction (SSI) effect in these bridges by comparing the identified and physical parameters.

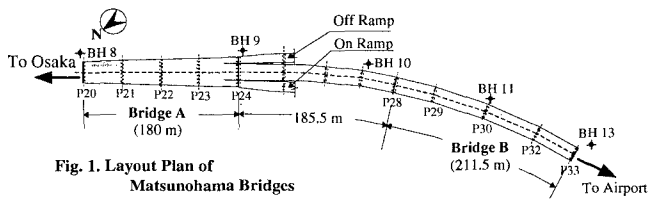

Fig. 1. Layout Plan of Matsunohama Bridges

2- System Identification Methodology: The system identification method developed by the authors consists of two steps. Firstly, modal parameters of the non-classically damped system are identified by using the free field acceleration as input and accelerations at pier cap and girder as the output. Later, the structural parameters are identified by a global search scheme such that the normalized error between the identified and structural frequencies and damping ratios is minimized.

3- Matsunohama Viaduct Bridges: Matsunohama Viaduct on the Wangan route of the Hanshin Expressway incorporates special earthquake resistant design features as some of its spans are supported by base isolation bearings. The viaduct has two base isolated bridges within a distance of 185 m as shown in Fig. 1. Both bridges are 4-span continuous bridges. Bridge A has a steel I-girder super-structure which is supported on laminated rubber bearings on the interior piers and Teflon sliding bearings at the end piers. Whereas the two non-composite steel box girders of Bridge B are supported by lead rubber bearings on the interior piers and pivot roller bearings at the end piers. The bridges were excited by one main shock and four aftershocks of the 1995 Kobe earthquake whose summary is presented in Table 1. Pier P23 of Bridge A and P32 of Bridge B is instrumented at four locations as shown in Fig. 2a. A 2DOF lumped mass model is selected to represent the dynamics of the bridge in the longitudinal direction as depicted in Fig. 2b.

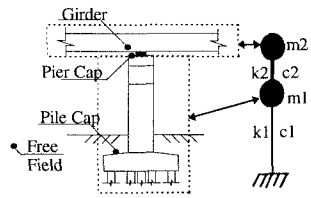

Fig. 2a. Accelerometer Location at P23 & P32

Fig. 2b. 2DOF Model of the Bridge

Table 1: Summary of recorded earthquakes

Earthquake	Maximum Acceleration (cm/s²)			
	Bridge A		Bridge B	
	Free field	*Pier cap*	*Free field*	*Pier cap*
Main Shock	149	226	136	201
Aftershock 1	20	22	20	16
Aftershock 2	13	40	18	28
Aftershock 3	5	9	4	3
Aftershock 4	20	27	12	17

4- Physical Modeling

a) Seismic response analysis of site and pile group impedance: The sub-structure consists of reinforced concrete piers supported on 1.2m diameter cast-in-situ reinforced concrete piles. Number, length and arrangement of piles vary for all piers of both bridges. Soil properties were found from SPT logs of bore holes 8 and 9 for Bridge A and from bore holes 10, 11 and 13 for Bridge B. Shear strain compatible dynamic shear wave velocity, soil shear modulus and soil damping ratio were determined by conducting a deconvolution analysis by computer program SHAKE91 [2]. Results of this analysis are shown in Table 2. These soil parameters were then used to compute horizontal and rocking dynamic pile group impedance according to the procedure of Dobry and Gazetas [3]. Kinematic interaction and frequency dependence of pile group impedance were found to have negligible effect up to the frequency of interest (<5 Hz.) and thus were ignored.

Table 2. Dynamic Soil Parameters during Earthquakes

Earthquake	Soil Shear Modulus (MPa)					Soil Damping Ratio (%)				
	BH 8	BH 9	BH 10	BH 11	BH 13	BH 8	BH 9	BH 10	BH 11	BH 13
Main Shock	124.73	100.72	82.70	72.56	63.46	5.97	5.92	6.66	7.26	7.33
Aftershock 1	191.62	139.61	116.53	124.12	97.57	1.89	2.18	2.42	2.12	2.55
Aftershock 2	196.49	142.41	119.38	129.51	100.76	1.71	1.94	2.12	1.74	2.18
Aftershock 3	202.21	145.23	123.12	137.82	104.83	1.33	1.65	1.58	0.93	1.64
Aftershock 4	193.10	140.23	118.80	128.30	100.22	1.90	2.12	2.17	1.80	2.25

b) Stiffness of reinforced concrete columns: Actual stiffness of a bridge column can be found from the theoretical load vs. deflection curves and the actual recorded deflection. Theoretical deflection, Δ, can be determined by integrating the theoretical curvatures and shear strains over the entire height of the column for a particular value of lateral load, P. Theoretical moment-curvature and shear strain vs. shear stress relationships for sections subjected to combined axial load, moment and shear force were found by computer program RESPONSE-2000 [4]. Stiffness of all columns was calculated as secant stiffness from the theoretical P-Δ curves for the maximum recorded pier cap displacement relative to the pile cap.

5- Comparison of Identified and Physical Sub-structure Parameters

a) Sub-structure stiffness: To clarify the SSI effect, the identified values of the sub-structure stiffness were compared with the

Key words: soil-structure interaction, system identification, pile foundation, Kobe earthquake, base-isolated bridge
Address: 7-3-1 Hongo, Bunkyo-ku, Tokyo 113-8656, Japan. Tel: 03-5802-3312, Fax: 03-5689-7292

equivalent physical sub-structure stiffness which consisted of three components viz. horizontal & rocking pile group stiffness and concrete column stiffness as shown in Fig. 3. Therefore, equivalent physical sub-structure stiffness can be represented as $k_{sub} = k_c k_h k_r' / \left(k_c (k_h + k_r') + k_h k_r'\right)$ where k_c is stiffness of column, k_h is horizontal stiffness of pile group and k_r', rocking stiffness of pile group converted to equivalent horizontal stiffness for unit rotation. Comparison of the identified and physical sub-structure stiffness is shown in Fig. 4 along with the case of a fixed base for both bridges. It can be observed that the identified value is in agreement with the physical one for both bridges. It should be noted that for Bridge A, the identified and physical values are nearly equal to the fixed base case while for Bridge B, the fixed base stiffness value is nearly twice the identified value. This suggests that the effect of SSI is more pronounced at Bridge B. This is attributed to weaker soil at Bridge B and the fact that number of piles per pier is less for this bridge.

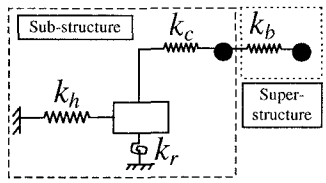

Fig. 3. Components of Stiffness

b) Components of sub-structure compliance: Contribution of each component of sub-structure stiffness to the overall sub-structure stiffness is investigated by looking at the compliance of the system which is the inverse of stiffness and is given as $f_{sub} = f_c + f_h + f_r'$, where f_c, f_h and f_r' are the inverse of k_c, k_h and k_r'. Fig. 5 shows the share of each component during all earthquakes based on the physical model. Maximum contribution to compliance comes from the column while the rest is due to the horizontal pile group compliance with negligible contribution coming from the rocking compliance. This implies that the rocking stiffness of the pile groups is so high that it contributes little to the dynamics of both bridges. The share of horizontal pile group compliance increases from about 10% in Bridge A to about 40% in Bridge B indicating a larger contribution of SSI in Bridge B.

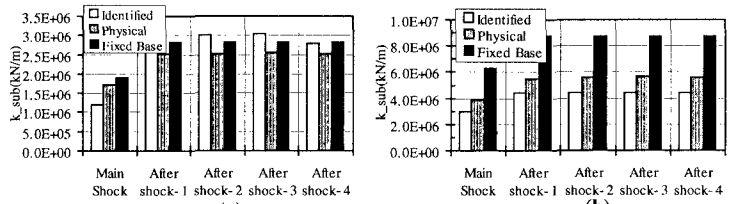

Fig. 4. Comparison of Sub-structure Stiffness. (a) Bridge A, (b) Bridge B

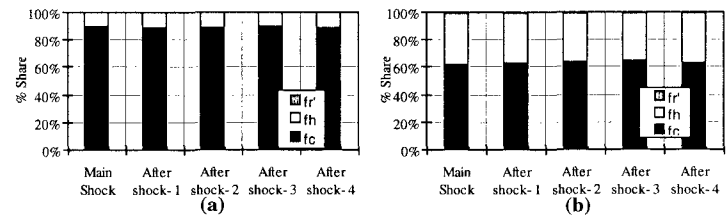

Fig. 5. Components of Compliance. (a) Bridge A, (b) Bridge B

c) Variation of soil shear modulus and shear strain during earthquakes: Variation of soil shear modulus, computed by SHAKE91, during earthquakes is plotted in Fig. 6. Maximum reduction in soil shear modulus was observed for bore hole 11 where its value was about 50% of the small strain value corresponding to soil shear strain of 0.024%. Fig. 7 depicts the relationship between soil shear strain and normalized soil shear modulus. This range of dynamic soil parameters is similar to the observation of Kokusho et al.[5].

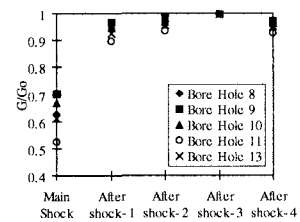

Fig. 6. Variation of G/G_0 during Earthquakes

6- Conclusions: This study shows that it is possible to capture the overall behavior of the Matsunohama viaduct bridges with a simple 2DOF lumped mass model. It is observed that the identified sub-structure stiffness is nearly equal to the physical sub-structure stiffness calculated by considering SSI. Effect of SSI is pronounced in Bridge B as the identified sub-structure stiffness is almost half the fixed base stiffness and the share of horizontal pile group compliance is significant. This implies that ignoring the effect of SSI arising from horizontal pile group stiffness will introduce considerable error in the analysis of Bridge B. Whereas rocking pile group compliance has a negligible contribution in both bridges. Reduction in the soil shear modulus during the main shock is more as compared to the aftershocks.

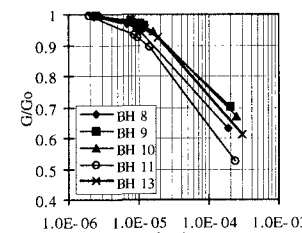

Fig. 7. Soil Shear Strain vs. G/G_0 Relationship

Acknowledgments: The authors are thankful to Dr. M. Kitazawa, H. Kobayashi and H. Mizutani of Hanshin Expressway Public Corporation for providing the strong motion records and construction drawings of Matsunohama Viaduct bridges and valuable comments during the study.

References: **[1]** Chaudhary, M.T.A., Abe, M., Fujino, Y. and Yoshida J. (1999)," System identification and performance evaluation of a base-isolated bridge during the 1995 Kobe earthquake", *Proceedings of 13th ASCE Engineering Mechanics Conference,* Baltimore, USA, (accepted). **[2]** Idriss, I.M. and Sun, J.I. (1992). "SHAKE91: A computer program for conducting equivalent linear seismic response analyses of horizontally layered soil deposits", User's guide, University of California, Davis, 13 pp. **[3]** Dobry, R. and Gazetas, G.(1988). "Simple method for dynamic stiffness and damping of floating pile groups", *Geotechnique,* 38(4),557-574. **[4]** Bentz, E. (1999). "RESPONSE-2000: Load-deformation response of reinforced concrete sections", *Ph.D. Dissertation,* Department of Civil Engineering, University of Toronto. **[5]** Kokusho, T., Sato, K., and Matsumoto, M. (1996). "Nonlinear dynamic soil properties back-calculated from strong seismic motions during Hyogoken-Nanbu earthquake", *Proceedings of the 11th World Conference on Earthquake Engineering,* Acapulco, Paper No. 2080.